

Supporting Information

Ba₂[WO₃F(IO₃)][WO₃F₂]: The First Polar Fluorinated Tungsten Iodate Featuring the Direct W-O-I Bond

Ying Hou,^{‡a} Hongyi Li,^{‡b} Hongping Wu,^{a,*} Hongwei Yu,^a Zhanggui Hu,^a Jiyang Wang,^a Yicheng Wu^a

^aTianjin Key Laboratory of Functional Crystal Materials, Institute of Functional Crystals, Tianjin University of Technology, Tianjin 300384, China.

^bGuangzhou Panyu Polytechnic, Guangdong 511483, China.

CONTENTS

Experimental Details	S1
Table S1. Crystal data and structure refinement for Ba ₂ [WO ₃ F(IO ₃)][WO ₃ F ₂].....	S4
Table S2. Atoms coordinates, equivalent isotropic displacement parameters for Ba ₂ [WO ₃ F(IO ₃)][WO ₃ F ₂]	S5
Table S3. Selected bond distances (Å) and angles (deg) for Ba ₂ [WO ₃ F(IO ₃)][WO ₃ F ₂]	S6
Table S4. Dipole Moment Direction and Magnitude (in Debye) S9	
Fig. S1 X-ray powder diffraction patterns of Ba ₂ [WO ₃ F(IO ₃)][WO ₃ F ₂].	S10
Fig. S2 EDS spectrum of Ba ₂ [WO ₃ F(IO ₃)][WO ₃ F ₂].....	S10
Fig. S3 ORTEP drawing of the asymmetric unit.	S10
Fig. S4 XRD diagram of the residual after TG/DSC of Ba ₂ [WO ₃ F(IO ₃)][WO ₃ F ₂]	S11
Fig. S5 The band gap of of Ba ₂ [WO ₃ F(IO ₃)][WO ₃ F ₂]......	S11
Fig. S6 The infrared spectrum of Ba ₂ [WO ₃ F(IO ₃)][WO ₃ F ₂]......	S11
Fig. S7 The direction of dipole moments of Ba ₂ [WO ₃ F(IO ₃)][WO ₃ F ₂]	S12
Fig. S7 Birefringence curve of Ba ₂ [WO ₃ F(IO ₃)][WO ₃ F ₂].	S12
Fig. S8 Crystal size photo of Ba ₂ [WO ₃ F(IO ₃)][WO ₃ F ₂]	S12

Experimental Details

Reagents

Iodine pentoxide (I_2O_5 , 98%, Shanghai Aladdin Chemistry Co., Ltd.), tungsten trioxide (WO_3 , 99.0%, Tianjin Kemiou Chemical Reagent Co., Ltd.), and barium fluoride (BaF_2 , 99%, Shanghai Aladdin Chemistry Co., Ltd.) were commercially available and used as received.

Hydrothermal Synthesis

The starting reagents are 0.297 g (0.80×10^{-3} mol) of I_2O_5 , 0.372 g (1.60×10^{-3} mol) of WO_3 , 0.298g (1.70×10^{-3} mol) of BaF_2 . The mixture of the starting materials was placed into a 23 ml Parr autoclave with 3.5 ml of deionized water as backfills. The autoclave was quickly heated to 220 °C, held for 70 h and cooled to the room temperature at 3 °C/h. After the reaction, the products were washed with deionized water and dried in air. The colorless single crystals of $Ba_2[WO_3F(IO_3)][WO_3F_2]$ were obtained. F⁻ is difficult to introduce into iodate salts. First, early transition-metal (W) has been introduced to iodate, thus F can be introduced to iodate as a ligand of W. Generally speaking, hydrofluoric acid is often required to provide an acidic environment and increases the solubility of water-insoluble substance. However, the raw materials are I_2O_5 , WO_3 and BaF_2 . I_2O_5 , which can be dissolved in water and become HIO_3 to provide acidic conditions. In addition, the method of high temperature and high pressure is adopted to promote the dissolution of WO_3 . Thus, raw materials in this paper can achieve the same effect as HF acid.

Energy-Dispersive Spectroscopy (EDS)

Microprobe elemental analyses and the elemental distribution map was performed using an energy dispersive X-ray spectroscope (EDS) with a field-emission scanning electron microscope (Quanta FEG 250) made by FEI. The average atomic ratio in $Ba_2[WO_3F(IO_3)][WO_3F_2]$ was Ba: W: I: O: F = 11.77: 11.43: 5.08: 52.99: 18.73, which was approximately equal to the theoretical one, 2: 2: 1: 9: 3.

Single-Crystal X-ray Diffraction

A Bruker SMART APEX II 4K CCD diffractometer with Mo-K α radiation ($\lambda = 0.71073$ Å) was used to collect the single-crystal XRD data at 296(2) K, and the data were

integrated with a SAINT program. The crystal structure was solved by the direct method, and refined by the SHELXTL system. All of the atomic positions were refined by full matrix least-squares techniques. The structure was checked for missing symmetry elements with PLATON. The crystal data and structural refinement information are summarized in Table S1. The atomic coordinates and the equivalent isotropic displacement parameters are available in Table S2. The selected bond lengths and angles are listed in Table S3.

Powder X-ray Diffraction

Inspection of polycrystalline powder purity of $\text{Ba}_2[\text{WO}_3\text{F}(\text{IO}_3)][\text{WO}_3\text{F}_2]$ was carried out with a Bruker D2 PHASER powder X-ray diffractometer equipped with Cu-K α radiation ($\lambda = 1.5418 \text{ \AA}$). During the powder diffraction procedure, the angular range and the fixed scanning step were maintained at the constant value of $2\theta = 10^\circ - 70^\circ$, and 1s/step, respectively. The XRD patterns are displayed in Figure S1. It indicates that the experimental powder X-ray diffraction pattern of $\text{Ba}_2[\text{WO}_3\text{F}(\text{IO}_3)][\text{WO}_3\text{F}_2]$ agrees well with the theoretical one inferred from the crystallographic information file (cif).

Infrared Spectroscopy

The IR spectra of $\text{Ba}_2[\text{WO}_3\text{F}(\text{IO}_3)][\text{WO}_3\text{F}_2]$ was recorded on a Nicolet iS50 Fourier transform infrared instrument in the range of 400–4000 cm^{-1} . A sample of 10 mg was used for testing.

UV-vis-NIR diffuse reflectance spectroscopy

The UV–Vis–NIR diffuse reflectance spectrum was measured with a Shimadzu SolidSpec-3700DUV UV–vis–NIR spectrophotometer at room temperature. The measurement range was from 240 to 2500 nm, and the barium sulfate is used as the diffuse reflection standard. Absorption (K/S) data was calculated from the following Kubelka–Munk function: $F(R) = (1-R)^2/2R = K/S$, R represents the reflectance, K represents the absorption, and S represents the scattering factor.

Thermal Stability

The NETZSCH STA 449C thermal analysis instrument was employed to specify the thermal habits of $\text{Ba}_2[\text{WO}_3\text{F}(\text{IO}_3)][\text{WO}_3\text{F}_2]$. With the aid of in flowing nitrogen atmosphere condition, powder sample (~0.001 g) was heated from 20 to 1000 °C at the

constant rate of 5 °C/min.

Powder SHG Test

The Kurtz–Perry method was adopted to assess the SHG performance of Ba₂[WO₃F(FO₃)][WO₃F₂]. Polycrystalline powder of Ba₂[WO₃F(FO₃)][WO₃F₂] was classified into several different standard sizes: 25-53, 53-75, 75-106, 106-120, 120-150, 150-180 and 180-212 μm and KDP was served as a standard during the SHG test procedure. The polycrystalline sample was irradiated with a pulsed infrared beam produced by a Q-switched Nd: YAG laser.

Table S1. Crystal data and structure refinement for Ba₂[WO₃F(FO₃)][WO₃F₂].

Empirical formula	Ba ₂ [WO ₃ F(FO ₃)][WO ₃ F ₂]
Formula weight	970.28
Temperature	273 (2) K
Wavelength	0.71073 Å
Crystal system	Monoclinic
Space group	<i>Cc</i>
	<i>a</i> = 7.691(6) Å
Unit cell dimensions	<i>b</i> = 20.655(13) Å
	<i>c</i> = 7.418(5) Å
	β = 120.89(2) °
Volume	1011.3(12) Å ³
Z	4
Density (g/cm ³)	6.373
F(000)	1648
Theta range for data collection	1.972 to 27.503°
Limiting indices	-9≤h≤9, -25≤k≤25, -9≤l≤9
Reflections collected / unique	10127 / 2492
Reflections collected	10267
Reflections collected / unique	9200 / 1988 [R(int) = 0.0674]
Completeness to theta = 25.242°	100.0 %
Refinement method	Full-matrix least-squares on <i>F</i> ²
Data / restraints / parameters	1988 / 2 / 154
Goodness-of-fit on <i>F</i> ²	1.046
Final <i>R</i> indices [<i>F</i> _o ² >2σ(<i>F</i> _o ²)] ^[a]	<i>R</i> ₁ = 0.0346 <i>wR</i> ₂ = 0.0566
<i>R</i> indices (all data) ^[a]	<i>R</i> ₁ = 0.0413 <i>wR</i> ₂ = 0.0591
Absolute structure parameter	0.004(12)
Largest diff. peak and hole	1.584 and -1.236 e·Å ⁻³
[a] <i>R</i> ₁ = Σ <i>F</i> _o - <i>F</i> _c /Σ <i>F</i> _o and <i>wR</i> ₂ = [Σ <i>w</i> (<i>F</i> _o ² - <i>F</i> _c ²) ² / Σ <i>w</i> <i>F</i> _o ⁴] ^{1/2} for <i>F</i> _o ² > 2σ(<i>F</i> _o ²)	

Table S2. Atomic coordinates ($\times 10^4$) and equivalent isotropic displacement parameters ($\text{\AA}^2 \times 10^3$) for Ba₂[WO₃F(FO₃)][WO₃F₂] U(eq) is defined as one third of the trace of the orthogonalized Uij tensor.

Atoms	x	y	z	U(eq)	BVS
W(1)	7003(1)	5118(1)	5907(1)	23(1)	6.22
W(2)	2890(1)	7548(1)	3957(1)	33(1)	5.94
Ba(1)	1527(2)	5748(1)	1208(2)	26(1)	2.05
Ba(2)	3262(2)	8220(1)	9465(2)	33(1)	1.72
I(1)	3853(2)	3933(1)	2561(2)	28(1)	5.01
F(1)	8252(15)	4210(4)	6974(15)	30(2)	0.90
F(2)	1760(18)	6697(5)	3815(18)	42(3)	1.12
F(3)	3879(17)	7186(5)	2176(18)	45(3)	0.96
O(1)	3741(15)	8349(5)	3589(16)	21(3)	1.68
O(2)	5573(16)	5800(5)	4513(17)	22(3)	1.97
O(3)	6884(17)	5236(5)	8311(19)	26(3)	2.05
O(4)	333(19)	7693(6)	1247(19)	38(3)	2.09
O(5)	1696(19)	7842(5)	5404(19)	33(3)	1.63
O(6)	2146(19)	3439(6)	2910(20)	35(3)	2.15
O(7)	2294(18)	4493(5)	513(18)	27(3)	2.19
O(8)	4417(18)	4495(6)	4773(19)	33(3)	2.14
O(9)	9460(15)	5394(5)	6886(18)	26(3)	2.07

Table S3. Selected bond distances (Å) and angles (deg) for Ba₂[WO₃F(FO₃)][WO₃F₂].

W(1)-O(9)	1.736(10)	Ba(1)-O(7)#10	2.977(12)
W(1)-O(2)	1.759(10)	Ba(1)-O(9)#9	3.027(11)
W(1)-O(3)	1.848(12)	Ba(1)-O(6)#1	3.197(13)
W(1)-O(3)#1	2.018(12)	Ba(1)-O(3)#8	3.257(12)
W(1)-F(1)	2.070(9)	Ba(1)-W(1)#9	3.816(3)
W(1)-O(8)	2.145(11)	Ba(2)-O(5)	2.722(12)
W(2)-O(5)	1.837(12)	Ba(2)-F(1)#11	2.754(10)
W(2)-O(4)#5	1.840(12)	Ba(2)-O(6)#12	2.797(13)
W(2)-O(1)	1.850(10)	Ba(2)-F(3)#13	2.802(11)
W(2)-F(2)	1.939(10)	Ba(2)-O(1)#13	2.900(11)
W(2)-F(3)	1.979(11)	Ba(2)-O(2)#14	2.907(10)
W(2)-O(4)	1.985(12)	Ba(2)-F(2)#5	2.972(11)
Ba(1)-F(2)	2.695(10)	Ba(2)-F(3)#14	3.012(11)
Ba(1)-O(1)#7	2.751(10)	Ba(2)-O(5)#5	3.222(12)
Ba(1)-O(7)	2.764(11)	Ba(2)-O(9)#14	3.251(12)
Ba(1)-O(2)	2.806(11)	Ba(2)-O(4)#13	3.327(15)
Ba(1)-O(9)#8	2.847(11)	I(1)-O(6)	1.784(12)
Ba(1)-F(1)#9	2.854(10)	I(1)-O(7)	1.793(11)
Ba(1)-O(8)#1	2.959(12)	I(1)-O(8)	1.870(11)
O(9)-W(1)-O(2)	101.6(5)	O(8)#1-Ba(1)-O(6)#1	51.7(3)
O(9)-W(1)-O(3)	97.8(5)	O(7)#10-Ba(1)-O(6)#1	152.0(3)
O(2)-W(1)-O(3)	97.8(5)	O(9)#9-Ba(1)-O(6)#1	146.5(3)
O(9)-W(1)-O(3)#1	91.4(5)	F(2)-Ba(1)-O(3)#8	110.9(3)
O(2)-W(1)-O(3)#1	91.2(5)	O(1)#7-Ba(1)-O(3)#8	64.0(3)
O(3)-W(1)-O(3)#1	165.5(3)	O(7)-Ba(1)-O(3)#8	80.8(3)
O(9)-W(1)-F(1)	86.9(5)	O(2)-Ba(1)-O(3)#8	159.6(3)
O(2)-W(1)-F(1)	167.8(4)	O(9)#8-Ba(1)-O(3)#8	52.0(3)
O(3)-W(1)-F(1)	89.6(4)	F(1)#9-Ba(1)-O(3)#8	50.2(3)
O(3)#1-W(1)-F(1)	79.7(4)	O(8)#1-Ba(1)-O(3)#8	118.6(3)
O(9)-W(1)-O(8)	162.1(5)	O(7)#10-Ba(1)-O(3)#8	101.5(3)
O(2)-W(1)-O(8)	94.4(5)	O(9)#9-Ba(1)-O(3)#8	50.6(3)
O(3)-W(1)-O(8)	87.8(5)	O(6)#1-Ba(1)-O(3)#8	102.1(3)
O(3)#1-W(1)-O(8)	80.2(5)	O(5)-Ba(2)-F(1)#11	67.9(3)

F(1)-W(1)-O(8)	76.2(4)	O(5)-Ba(2)-O(6)#12	135.7(4)
O(5)-W(2)-O(4)#5	97.5(6)	F(1)#11-Ba(2)-O(6)#12	97.3(3)
O(5)-W(2)-O(1)	96.4(5)	O(5)-Ba(2)-F(3)#13	113.0(4)
O(4)#5-W(2)-O(1)	96.1(5)	F(1)#11-Ba(2)-F(3)#13	171.4(3)
O(5)-W(2)-F(2)	89.2(5)	O(6)#12-Ba(2)-F(3)#13	76.1(3)
O(4)#5-W(2)-F(2)	91.3(5)	O(5)-Ba(2)-O(1)#13	159.8(4)
O(1)-W(2)-F(2)	170.0(5)	F(1)#11-Ba(2)-O(1)#13	126.5(3)
O(5)-W(2)-F(3)	173.5(5)	O(6)#12-Ba(2)-O(1)#13	61.5(3)
O(4)#5-W(2)-F(3)	87.3(5)	F(3)#13-Ba(2)-O(1)#13	55.2(3)
O(1)-W(2)-F(3)	87.3(5)	O(5)-Ba(2)-O(2)#14	107.5(3)
F(2)-W(2)-F(3)	86.4(5)	F(1)#11-Ba(2)-O(2)#14	74.6(3)
O(5)-W(2)-O(4)	90.5(6)	O(6)#12-Ba(2)-O(2)#14	108.0(3)
O(4)#5-W(2)-O(4)	170.7(6)	F(3)#13-Ba(2)-O(2)#14	112.4(3)
O(1)-W(2)-O(4)	87.6(5)	O(1)#13-Ba(2)-O(2)#14	68.2(3)
F(2)-W(2)-O(4)	84.2(5)	O(5)-Ba(2)-F(2)#5	76.1(3)
F(3)-W(2)-O(4)	84.4(5)	F(1)#11-Ba(2)-F(2)#5	62.6(3)
F(2)-Ba(1)-O(1)#7	75.8(3)	O(6)#12-Ba(2)-F(2)#5	60.5(3)
F(2)-Ba(1)-O(7)	150.9(3)	F(3)#13-Ba(2)-F(2)#5	109.0(3)
O(1)#7-Ba(1)-O(7)	131.9(3)	O(1)#13-Ba(2)-F(2)#5	122.0(3)
F(2)-Ba(1)-O(2)	73.1(3)	O(2)#14-Ba(2)-F(2)#5	132.1(3)
O(1)#7-Ba(1)-O(2)	134.7(3)	O(5)-Ba(2)-F(3)#14	64.2(3)
O(7)-Ba(1)-O(2)	87.2(3)	F(1)#11-Ba(2)-F(3)#14	102.2(3)
F(2)-Ba(1)-O(9)#8	142.0(3)	O(6)#12-Ba(2)-F(3)#14	157.1(3)
O(1)#7-Ba(1)-O(9)#8	66.2(3)	F(3)#13-Ba(2)-F(3)#14	85.5(2)
O(7)-Ba(1)-O(9)#8	66.3(3)	O(1)#13-Ba(2)-F(3)#14	96.9(3)
O(2)-Ba(1)-O(9)#8	136.2(3)	O(2)#14-Ba(2)-F(3)#14	66.6(3)
F(2)-Ba(1)-F(1)#9	64.9(3)	F(2)#5-Ba(2)-F(3)#14	140.3(3)
O(1)#7-Ba(1)-F(1)#9	70.9(3)	O(5)-Ba(2)-O(5)#5	83.8(2)
O(7)-Ba(1)-F(1)#9	111.1(3)	F(1)#11-Ba(2)-O(5)#5	111.7(3)
O(2)-Ba(1)-F(1)#9	121.4(3)	O(6)#12-Ba(2)-O(5)#5	62.6(3)
O(9)#8-Ba(1)-F(1)#9	101.1(3)	F(3)#13-Ba(2)-O(5)#5	60.5(3)
F(2)-Ba(1)-O(8)#1	126.6(3)	O(1)#13-Ba(2)-O(5)#5	100.9(3)
O(1)#7-Ba(1)-O(8)#1	108.5(3)	O(2)#14-Ba(2)-O(5)#5	168.7(3)
O(7)-Ba(1)-O(8)#1	60.1(3)	F(2)#5-Ba(2)-O(5)#5	50.5(3)
O(2)-Ba(1)-O(8)#1	67.7(3)	F(3)#14-Ba(2)-O(5)#5	119.2(3)

O(9)#8-Ba(1)-O(8)#1	68.9(3)	O(5)-Ba(2)-O(9)#14	134.7(3)
F(1)#9-Ba(1)-O(8)#1	168.4(3)	F(1)#11-Ba(2)-O(9)#14	67.6(3)
F(2)-Ba(1)-O(7)#10	56.5(3)	O(6)#12-Ba(2)-O(9)#14	59.0(3)
O(1)#7-Ba(1)-O(7)#10	121.6(3)	F(3)#13-Ba(2)-O(9)#14	112.3(3)
O(7)-Ba(1)-O(7)#10	95.7(2)	O(1)#13-Ba(2)-O(9)#14	59.3(3)
O(2)-Ba(1)-O(7)#10	63.2(3)	O(2)#14-Ba(2)-O(9)#14	51.8(3)
O(9)#8-Ba(1)-O(7)#10	148.6(3)	F(2)#5-Ba(2)-O(9)#14	90.9(3)
F(1)#9-Ba(1)-O(7)#10	60.0(3)	F(3)#14-Ba(2)-O(9)#14	118.3(3)
O(8)#1-Ba(1)-O(7)#10	125.9(3)	O(5)#5-Ba(2)-O(9)#14	120.8(3)
F(2)-Ba(1)-O(9)#9	107.2(3)	O(5)-Ba(2)-O(4)#13	109.9(3)
O(1)#7-Ba(1)-O(9)#9	111.1(3)	F(1)#11-Ba(2)-O(4)#13	137.8(3)
O(7)-Ba(1)-O(9)#9	58.7(3)	O(6)#12-Ba(2)-O(4)#13	108.2(3)
O(2)-Ba(1)-O(9)#9	109.0(3)	F(3)#13-Ba(2)-O(4)#13	50.6(3)
O(9)#8-Ba(1)-O(9)#9	87.1(2)	O(1)#13-Ba(2)-O(4)#13	49.9(3)
F(1)#9-Ba(1)-O(9)#9	53.0(3)	O(2)#14-Ba(2)-O(4)#13	65.9(3)
O(8)#1-Ba(1)-O(9)#9	118.9(3)	F(2)#5-Ba(2)-O(4)#13	159.6(3)
O(7)#10-Ba(1)-O(9)#9	61.5(3)	F(3)#14-Ba(2)-O(4)#13	48.9(3)

Symmetry transformations used to generate equivalent atoms:

#1 x,-y+1,z-1/2 #2 x+1,-y+1,z+1/2
#3 x+1/2,-y+3/2,z-1/2 #4 x+1,y,z+1
#5 x+1/2,-y+3/2,z+1/2 #6 x,y,z-1
#7 x-1/2,-y+3/2,z-1/2 #8 x-1,y,z-1
#9 x-1,-y+1,z-1/2 #10 x,-y+1,z+1/2
#11 x-1/2,y+1/2,z #12 x+1/2,y+1/2,z+1
#13 x,y,z+1 #14 x-1/2,-y+3/2,z+1/2
#15 x-1/2,y-1/2,z-1 #16 x+1/2,y-1/2,z

Table S4. Dipole Moment Direction and Magnitude (in Debye) of $[\text{WO}_4\text{F}_2]$, $[\text{WO}_5\text{F}]$ and $(\text{IO}_3)^-$ in $\text{Ba}_2[\text{WO}_3\text{F}(\text{IO}_3)][\text{WO}_3\text{F}_2]$.

species	a	b	c
$[\text{WO}_5\text{F}]^{5-}$	7.40	0	-0.99
$[\text{WO}_4\text{F}_2]^{5-}$	-2.12	0	-3.47
$(\text{IO}_3)^-$	-130.61	0	14.34

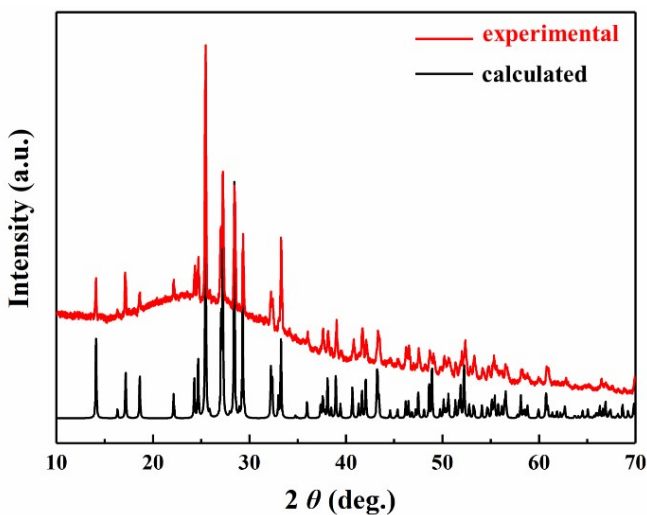


Fig. S1 X-ray powder diffraction patterns of $\text{Ba}_2[\text{WO}_3\text{F}(\text{IO}_3)][\text{WO}_3\text{F}_2]$.

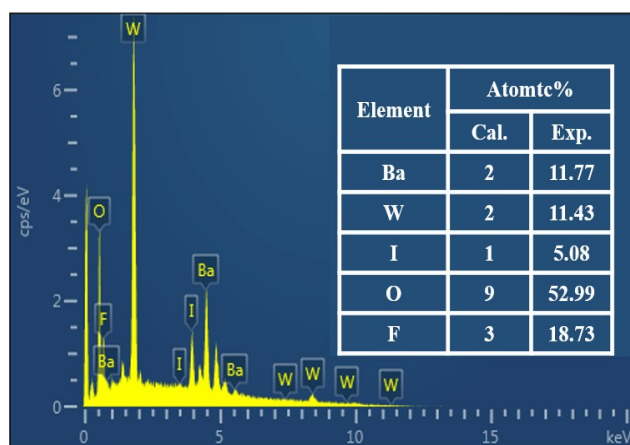


Fig. S2 EDS spectrum of $\text{Ba}_2[\text{WO}_3\text{F}(\text{IO}_3)][\text{WO}_3\text{F}_2]$.

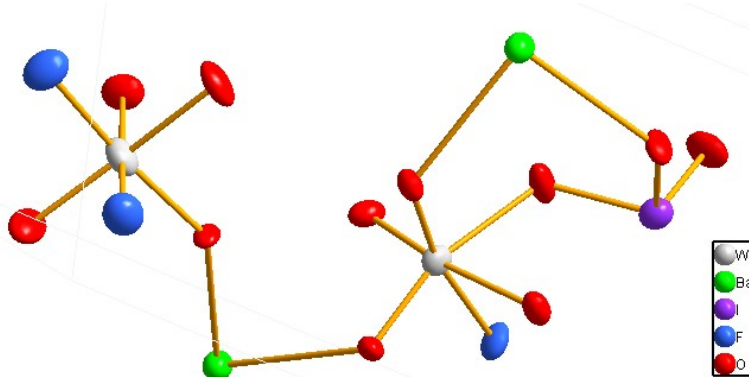


Fig. S3 ORTEP drawing of the asymmetric unit of $\text{Ba}_2[\text{WO}_3\text{F}(\text{IO}_3)][\text{WO}_3\text{F}_2]$. Thermal ellipsoids are drawn at a 50% probability level.

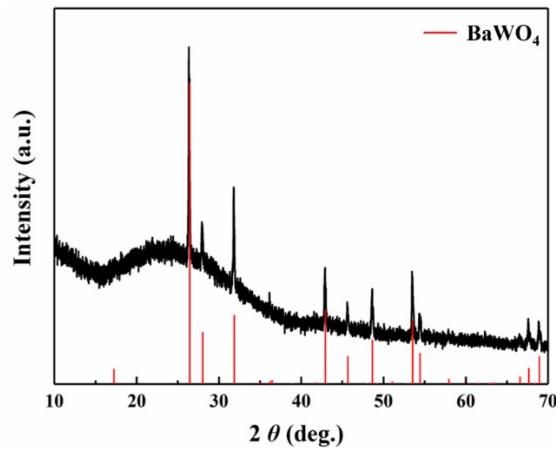


Fig. S4 XRD diagram of the residual after TG/DSC of $\text{Ba}_2[\text{WO}_3\text{F}(\text{IO}_3)]\text{[WO}_3\text{F}_2]$.

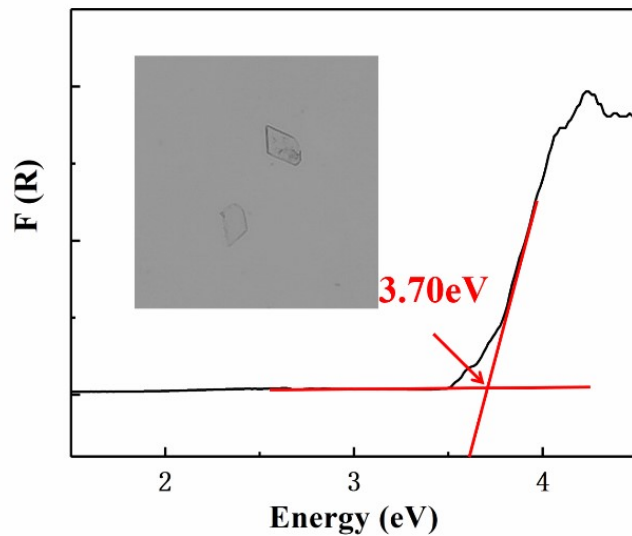


Fig. S5 The band gap of $\text{Ba}_2[\text{WO}_3\text{F}(\text{IO}_3)]\text{[WO}_3\text{F}_2]$.

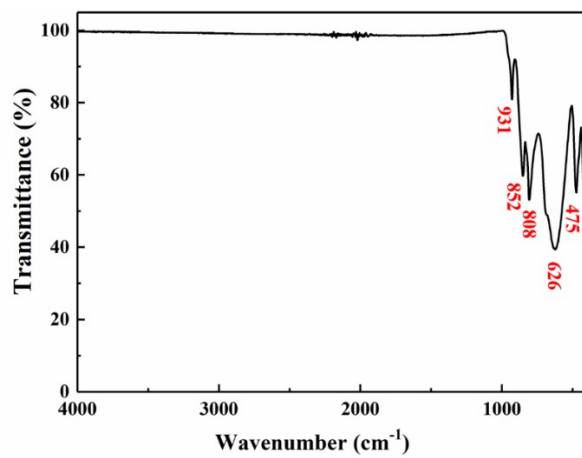


Fig. S6 The infrared spectrum of $\text{Ba}_2[\text{WO}_3\text{F}(\text{IO}_3)]\text{[WO}_3\text{F}_2]$.

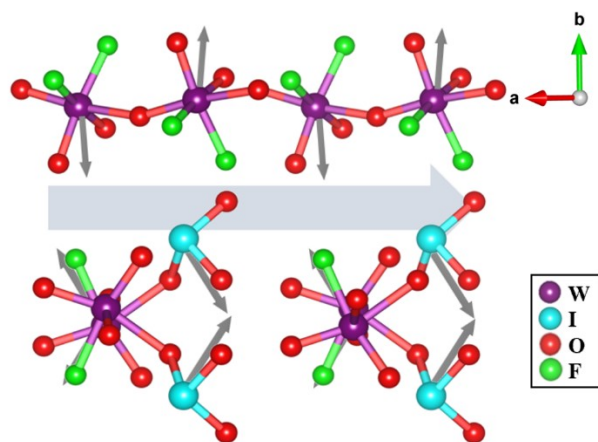


Fig. S7 The direction of dipole moments of $\text{Ba}_2[\text{WO}_3\text{F}(\text{IO}_3)][\text{WO}_3\text{F}_2]$.

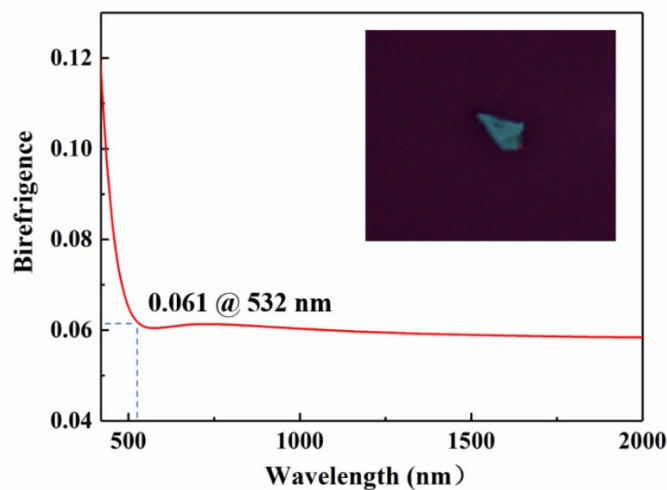


Fig. S8 Birefringence curve of $\text{Ba}_2[\text{WO}_3\text{F}(\text{IO}_3)][\text{WO}_3\text{F}_2]$.

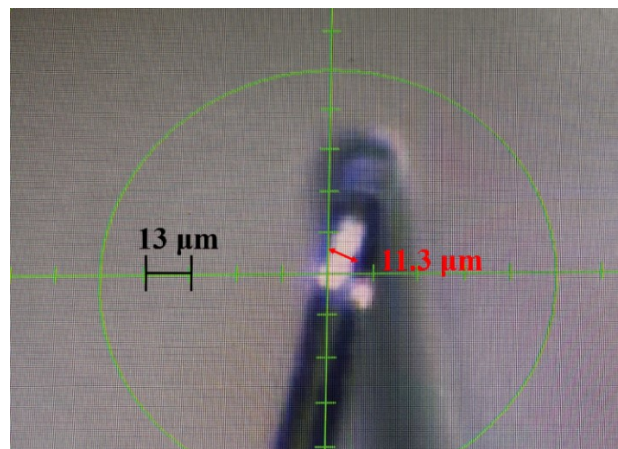


Fig. S9 Crystal size photo of $\text{Ba}_2[\text{WO}_3\text{F}(\text{IO}_3)][\text{WO}_3\text{F}_2]$.